# Comparison of doubly-excited helium energy levels, isoelectronic series, autoionization lifetimes, and group-theoretical configuration-mixing predictions with large-configuration-interaction calculations and experimental spectra*

David R. Herrick† and Oktay Sinanoğlu‡
*Sterling Chemistry Laboratory, Yale University, New Haven, Connecticut 06520*
(Received 6 August 1973; revised manuscript received 24 July 1974)

For comparison with our recent group-theoretical predictions of configuration-mixing coefficients, we report extensive configuration-interaction calculations for doubly excited states in the helium isoelectronic sequence below the $N = 2$ ($S, P, D$ states), $N = 3$ ($S,P,D,F,G$ states), $N = 4$ ($S,P,D$ states), and $N = 5$ ($^1P^o$ states) ionization thresholds. Two new quantum numbers label the Rydberg series, and are used to predict three "selection rules" for dipole excitation and autoionization processes which agree with experiment. New autoionization widths are reported for the helium states and confirm our group-theoretically predicted selection rules. Our width of 0.151 eV for the $^1P^o$ state at 62.92 eV is in agreement with the recent experimental value $0.132 \pm 0.014$ eV. Calculations of helium energies and autoionization widths are strongly affected by "avoided crossings" of the doubly excited states as $Z$ is varied continuously. The new quantum numbers project out states in $H^-$ which correspond to observed $^1P^o$ shape resonances above the $N = 2$ and 3 ionization thresholds.

## I. INTRODUCTION

We describe in the present paper a new classification of doubly-excited Rydberg series and autoionization widths in helium. The classification is an extension of a previous investigation[1] (referred to as [I]) in which we showed that "intrashell" mixings of two-electron degenerate hydrogenic configurations (e.g., $2s^2 : 2p^2\,{}^1S$) due to the Coulomb interaction $1/R_{12}$ can be predicted quite well (but not exactly) by a new group-theoretical technique. Specifically, the method involved the diagonalization of an operator $B^2 = (\vec{b}_1 - \vec{b}_2)$,[2] where $\vec{b}_1$ and $\vec{b}_2$ are proportional to the Runge-Lenz vector[2] for electrons 1 and 2, respectively. $B^2$ can be represented with the Lie-algebra generators of either SO(3,1) or SO(4), and its diagonalization subject to conservation of $\hat{L}^2, \hat{S}^2$, and parity ($=\pi$) is obtained naturally from irreducible representations of the respective Lie algebras. The resulting configuration mixed "doubly-excited symmetry basis" (DESB) is characterized by two new integer quantum numbers $K$ and $T$.

The DESB states did not describe accurately the "intershell" Coulomb mixings of degenerate hydrogenic configurations, which contain orbitals from different atomic shells (e.g., $2sns : 2pnp\,{}^1S$; $n \geq 3$). Our present investigation shows conclusively, however, that in larger configuration-interaction (CI) bases containing both intrashell and intershell hydrogenic configurations, the quantum numbers $K$ and $T$ are actually "good" labels for the states in the sense that each CI eigenvector is composed mainly of DESB states having the same values of $K$ and $T$. Although this approximate diagonalization of the CI energy matrix is not exact, the resulting "classification" of the doubly-excited states is quite good over the entire isoelectronic sequence (nuclear charge $Z \geq 1$).

The nonrelativistic two-electron Hamiltonian is

$$H = Z^2[(P_1^2 + P_2^2)/2 - 1/R_1 - 1/R_2] + Z/R_{12}, \qquad (1)$$

where $P_k$ and $R_k$ are the $Z$-weighted coordinates $p_k/Z$ and $Zr_k$, respectively. For $Z > 1$ the energy spectrum of (1) is conveniently described in terms of the successive ionization thresholds ($N = 1, 2, \ldots$), below each of which there is an "envelope" of Rydberg series. The lowest-energy envelope ($N = 1$) contains the singly-excited series $(1snL)^{2S+1}L^{\pi}$ approaching the first ionization threshold. Higher-energy Rydberg envelopes contain doubly-excited states, which in the usual spectroscopic notation are labeled $(Nl, nl')^{2S+1}L^{\pi}$ with $n = N, N+1, \ldots$. Each envelope contains an infinity of Rydberg series, and with successively higher values of $N$ the number of series for each $S$, $L$, and $\pi$ symmetry type increases rapidly. For instance, below the $N = 4$ threshold there are seven possible $^1P^o$ Rydberg series represented by the configurations $4snp$, $4pns$, $4pnd$, $4dnp$, $4dnf$, $4fnd$, $4fng$. The Coulomb interaction between these series is strong, and the resulting configuration-mixed series represent the actual physical states better than the single configurational representations.

The importance of such mixings in doubly-excited He was first cited by Cooper, Fano, and Prats[3] with their "±" classification of the $(2snp \pm 2pns)\,{}^1P^o$ Rydberg series. For the most part similar classifications of other Rydberg series have been found "empirically" by inspection of calculated CI eigenvectors and corresponding quantum defects in Rydberg formula fits to the ener-

gies. An excellent discussion of the more puzzling aspects of doubly-excited states has been presented by Fano.[4] Our use of the group theoretical DESB is the first successful attempt to classify *a priori* the types of configurational mixings found in the theoretical calculations.

The new classification also allows for the first time predictions of the relative "weakness"[4] of excitation or decay channels for the doubly-excited Rydberg series. Each doubly-excited state ($=\phi$) is degenerate with at least one singly ionized continuum state ($=\chi$). Subject to conservation of $L$, $S$, and $\pi$, the doubly-excited states can autoionize via the Coulomb interaction, and typically this radiationless transition $\phi \rightarrow \chi$ occurs within $10^{-15}$ to $10^{-10}$ seconds after creation of the state $\phi$. The only doubly-excited states not subject to Coulomb autoionization are the series $(2pnL)^{1,3}L^{\pi}(L=1,2,\ldots)$. Above the $N=2$ ionization threshold there are enough continuum channels to ensure that all states have a nonzero autoionization probability.

Experimental energies and lifetimes of autoionizing states have been obtained from uv absorption spectra[5,6] and a variety of particle impact techniques.[7-11] Reference 4 contains an extensive review of these methods. Recent observations[12-14] of autoionizing states in beam-foil spectra have yielded energies to within ±0.005 eV, although detection of radiation only from states with nonradiative widths less than $10^{-4}$ eV is currently possible.

By analyzing exchange and correlation properties of the DESB configurational mixings we make predictions of approximate uv excitation and autoionization "selection rules" which are in excellent agreement with experiment. New autoionization width calculations for helium are reported which also confirm the predictions.

## II. DESCRIPTION OF THE DESB AND OF HYDROGENIC CI ENERGY AND WIDTH CALCULATIONS

### A. Summary of the DESB

As shown in [I], the DESB Rydberg series are labeled with the quantum numbers $\{N, n, L, S, \pi, K, T\}$. $N$ and $n$ are the usual principal quantum numbers for the series members $n=N, N+1, \ldots$ below the $N$th ionization threshold. $K$ and $T$ are the new DESB quantum numbers. For each value of $L$, $T$ is restricted to the integers $T=0,1,\ldots,L$. In addition, if $\pi=(-)^{L+1}$ then $T>0$. The range of $K$ for each value of $T$ is $\pm K=N-T-1, N-T-3,\ldots,0$ or 1. The DESB configurational mixing is given by

$$|(Nn)KT^{2S+1}L^{\pi}\rangle=\sum_{l,l'}|Nl,nl';{}^{2S+1}L^{\pi}\rangle\, D^{KTL\pi}_{Nl,nl'}, \quad (2)$$

where $D$ is proportional to $9-j$ vector-coupling coefficients,

$$D^{KTL\pi}_{Nl,nl'}=(-)^{l'}[(P+T+1)(P-T+1)(2l+1)(2l'+1)]^{1/2} \times \begin{Bmatrix} \frac{1}{2}(N-1) & \frac{1}{2}(n-1) & \frac{1}{2}(P+T) \\ \frac{1}{2}(N-1) & \frac{1}{2}(n-1) & \frac{1}{2}(P-T) \\ l & l' & L \end{Bmatrix} M(T,\pi). \quad (3)$$

$P=n-1+K$, and $M$ is a normalization factor with $M=1$ if $T=0$; $M=\sqrt{2}$ if $T>0$; $M=0$ unless $(-)^{l+l'}=\pi$. For example, the $2sns$ and $2pnp$ $^{1,3}S^e$ hydrogenic configurations are mixed to give $(K,T)=(+1,0)$ states:

$$|(2n)+1\ 0\ {}^{1,3}S^e\rangle=\left[\frac{n+1}{2n}\right]^{1/2}|2sns\rangle+\left[\frac{n-1}{2n}\right]^{1/2}|2pnp\rangle, \quad (4)$$

and $(K,T)=(-1,0)$ states:

$$|(2n)-1\ 0\ {}^{1,3}S^e\rangle=\left[\frac{n-1}{2n}\right]^{1/2}|2sns\rangle-\left[\frac{n+1}{2n}\right]^{1/2}|2pnp\rangle. \quad (5)$$

The quantum number $T$ need be specified only for states with $L\geq 2$ and $N>2$, and we shall omit it in reference to $S$ and $P$ states.

### B. CI calculations

Energy eigenvalues and eigenvectors were calculated with a finite, unscreened, bound state hydrogenic CI basis consisting of the configurations $(Nl,nl')^{2S+1}L^{\pi}$ with $N$ fixed at a constant value $(N=2,3,4,5)$, and $N\leq n\leq 7$. Specific calculations include $S$, $P$, and $D$ states below the $N=2$ threshold; $S$, $P$, $D$, $F$, and $G$ states below the $N=3$ threshold; $S$, $P$, and $D$ states below $N=4$; and a single $^1P^o$ CI calculation for $N=5$. For example, the $N=2$ $^1P^o$ energies were obtained from diagonalization of the $16\times16$ energy matrix of the configurations $2s2p$, $2snp$, $2pns$, and $2pnd$ with $n=3-7$. Our CI basis is similar to that used by Altick and Moore[15] for $P^o$ and $D^e$ states below the $N=2$ threshold. The restriction that $N$ remain constant in each CI basis assures (i) the orthogonality of all eigenvectors belonging to different Rydberg envelopes, and (ii) the orthogonality of each eigenvector to lower threshold continuum channels $(N'l',kl)^{2S+1}L^{\pi}$, with $N'<N$. Here $N'l'$ represents a bound hydrogenic orbital and $kl$ is a continuum orbital. These orthogonality conditions remain valid even when no maximum on $n$ is imposed. Thus each CI energy is an upper bound to the exact Feshbach energy[16] $\epsilon_Q$ for the state. The exact resonance energy is $E=\epsilon_Q+\Delta$, where $\Delta$ is the

energy "shift." For $N>2$ our CI energies are quite close to accurate values of the $\epsilon_Q$. In many cases our results are actually closer to the experimental energies than are the more accurate calculations because $\Delta$ is positive. While we do not calculate any shifts, it is clear for $N>2$, that $\Delta$ cannot be neglected as it generally is for states below the $N=2$ threshold.

All CI calculations were repeated at a sufficient number of $Z$ values so that the effective quantum number $n^*$ in a Rydberg energy formula for each state could be represented as a smooth function of $Z^{-1}$ over the range $0 \leq Z^{-1} \leq 1$.

Each CI eigenvector ($\equiv \vec{c}$) was transformed to the DESB basis in order to determine the contribution to its normalization ($\equiv \vec{c} \cdot \vec{c}$) from all DESB states having the same values of $K$ and $T$. For instance, after transforming the lowest energy $^1S^e$ eigenvector of $Li^+(Z=3)$ to the DESB we find that 99.81% of its normalization is attributed to DESB states with $K=+1$, while only 0.19% of the normalization is due to DESB states with $K=-1$. We therefore "classify" the state as having quantum number $K=+1$.

### C. Width calculations

Autoionization widths were calculated for each $He(Z=2)$ CI state $\phi$ with the formula

$$\Gamma_i = 2\pi |(\phi|H|\chi_i)|^2, \tag{6}$$

where $\Gamma_i$ is the partial width for continuum channel $\chi_i$ ($i=1,2,\ldots$, number of channels). The $\chi_i$ were antisymmetrized products of a bound $He^+$ orbital and a screened Coulomb function. The total width $\Gamma$ of each state was determined by summing over all partial widths to continuum channels of lower thresholds. $\Gamma$ is of course invariant to any unitary transformation of the $\chi_i$.

Because of the large number of calculations performed, a full presentation of results is not possible here. We display only results of primary experimental interest, or which illustrate new features in the doubly-excited spectrum. A complete tabulation of energies ($Z=1,2,3,4$), widths ($Z=2$), as well as analytic expressions (in terms of $N$ and $n$) for many DESB mixing coefficients is available elsewhere.[17]

## III. AUTOIONIZATION AND UV EXCITATION "SELECTION RULES"

It is well known that Coulomb autoionization (AI) of doubly-excited states below the $N=2$ threshold can be described in terms of exchange effects[3,18] and the simultaneous penetration of the two electrons near the nucleus.[3,19] The exchange effects result from the Pauli exclusion principle, and Rydberg series not having a valence, or intrashell ($n=N$) state because of this effect are narrower than series in which the valence state is not excluded by the Pauli principle.[18] The two-electron density of a doubly-excited state in the nuclear region determines its overlap with the $1skL$ continuum state, and in turn the AI strength through Eq. (6). Wave functions which allow both electrons to approach the nucleus simultaneously lead to larger AI widths than those functions in which the radial motion of the electrons is out of phase. The DESB configuration mixings describe varied degrees of electron correlation in terms of $K$ and $T$. Predictions of approximate AI "selection rules" for Rydberg series can be made once the exchange and two-electron penetration properties of each state are expressed in terms of the DESB quantum numbers.

To this end we note that $L$, $n$, and $K$ in Eq. (2) are restricted so that $K \geq L-n+1$; otherwise the $9-j$ coefficients vanish. By setting $n=N$, a bound on the values of $K$ for which valence states exist is obtained:

*AI Rule I.* $K \geq L-N+1$.

The DESB states have definite exchange symmetry when $n=N$, and the requirement of antisymmetry imposes a second restriction on $K$ as follows:

*AI Rule II.* $l+l'+N+K+S =$ *an odd integer when* $n=N$.

Once $\pi$, $L$, $N$, and $S$ are specified, we predict that Rydberg series not satisfying Rules I and II are "AI-forbidden," while those which do satisfy the rules are relatively "AI-allowed." Neither rule contains explicit dependence upon the DESB quantum number $T$.

DESB states with the least positive values of $K$ and $T$ tend to orient the electrons toward the same side of the nucleus, while states with the most positive values of $K$ and $T$ orient the electrons towards opposite sides of the nucleus. This was demonstrated in [I] for the $2s^2:2p^2$ mixed DESB $^1S$ states in which the average value of $\cos\theta_{12}$ in the $K=\pm1$ state was $\mp\frac{3}{8}$. When the angular correlation of a wave function keeps the electrons toward opposite sides of the nucleus, it is easier for them to penetrate into the nuclear region simultaneously. We summarize this property as follows:

*AI Rule III.*

If more than one Rydberg series of definite $L$, $S$, and $\pi$ is allowed within either of the two autoionization classifications by Rules I and II, then series with $K \geq 0$ will be broader than series with $K<0$. If in addition, two AI-allowed series have the same value of $K$, then the one with the larger value of $T$ will be broader.

The same correlation effects which led to AI Rules I–III also allow us to predict the $^1P^o$ series below each ionization threshold which is most

strongly excited in dipole transitions from the ground state. It is readily seen that the resulting "selection rule" is that the doubly-excited $^1P^\circ$ series with $(K, T) = (N-2, 1)$ should predominate (and also have the largest AI width).

Since none of the preceding arguments explicitly depend upon $Z$, we expect that they will be correct over the entire isoelectronic sequence. Discussion of the validity of the AI rules is given in Sec. VI for $Z = 2$ only.

## IV. RESULTS OF CI CALCULATIONS AND DEMONSTRATION OF THE DESB CLASSIFICATION

The most important result of our analysis is that the DESB quantum numbers $K$ and $T$ remain good labels for the calculated doubly-excited states in the sense that the two-electron Hamiltonian is approximately block diagonalized with respect to $K$ and $T$ in our hydrogenic CI basis. This characterization of the eigenvectors is illustrated in Table I for the $P^\circ$ states of $Li^+$ below the $N = 2$ threshold. While $K$ and $T$ are not "exact" quantum numbers for the eigenvectors, the maximal $K$ and $T$ components are easily identified in each case. These results are typical of the classifications found for higher $N$ and $L$.

Plots of the effective Rydberg quantum number $n^*$ in Figs. 1–4 illustrate the DESB classification as a function of $Z$. The curves are highly symmetrical and each one can be labeled uniquely with the DESB quantum numbers $S$, $L$, $\pi$, $K$, $T$, $N$, and $n$, where $n$ is the limiting value of $n^*$ as $Z \to \infty$. For lower values of $Z$, the curves separate according to their $K$, $T$ labels, and when $Z \cong N$ the high energy states of level $n$ are nearly degenerate with the lower energy states of level $n+1$. The interaction between these states gives rise to "avoided crossings" of the curves, although the DESB classification on either side of the crossing is the same as if the crossing were exact. For purposes of classification we have indicated these regions as actual curve crossings, and to the extent that interactions nondiagonal in $K$ and $T$ can be ignored, the crossings are exact. Additional avoided crossings occur at lower $Z$ values, giving a very complicated curve structure for high $N$.

The position of the avoided crossings is crucial for the classification of the doubly-excited states, and in particular for the $N = 2$ states of He. An example of this is the intersection of the $K = +1_4$ and $K = -1_3$ curves of the $^1P^\circ$ series in Fig. 2 corresponding respectively to the $2s4p$-$2p4s$ and $2p3d$ states in the Cooper, Fano, and Prats notation. The symmetrical mixing of these two states is shown in Table II and indicates that the avoided crossing occurs at $Z > 2$ in our basis since the $+1_4$ state is lower in energy. A similar decomposition of the CI eigenvectors of Lipsky and Russek[20] into

TABLE I. Effective Rydberg quantum numbers and group-theoretical DESB classification of $N = 2$, $P^\circ$ states with $Z = 3$ from CI calculations with hydrogenic configurations $2snp$, $2pns$, $2pnd$ ($n = 2$–$7$). For instance, 99.05% of the lowest energy $^1P^\circ$ eigenvector is composed of zeroth-order DESB states with $K = 0$, $T = 1$. See also Fig. 2 at $Z = 3$.

| | | | Fraction of Normalization | | |
|---|---|---|---|---|---|
| | $K_n$ | $n^*$ | $K = +1$ | $K = 0$ | $K = -1$ |
| $^1P^\circ$ | $0_2$ | 1.796 | 0.0011 | 0.9905 | 0.0084 |
| | $1_3$ | 2.564 | 0.9906 | 0.0093 | 0.0001 |
| | $0_3$ | 2.953 | 0.0129 | 0.9610 | 0.0261 |
| | $-1_3$ | 3.209 | 0.0001 | 0.0281 | 0.9718 |
| | $1_4$ | 3.578 | 0.9765 | 0.0233 | 0.0002 |
| | $0_4$ | 3.975 | 0.0260 | 0.9186 | 0.0554 |
| | $-1_4$ | 4.209 | 0.0013 | 0.0565 | 0.9423 |
| $^3P^\circ$ | $1_2$ | 1.634 | 0.9994 | 0.0000 | 0.0006 |
| | $1_3$ | 2.694 | 0.9657 | 0.0325 | 0.0018 |
| | $0_3$ | 2.715 | 0.0324 | 0.9675 | 0.0001 |
| | $-1_3$ | 3.114 | 0.0019 | 0.0001 | 0.9980 |
| | $1_4$ | 3.698 | 0.9591 | 0.0382 | 0.0027 |
| | $0_4$ | 3.752 | 0.0373 | 0.9594 | 0.0033 |
| | $-1_4$ | 4.102 | 0.0039 | 0.0024 | 0.9937 |

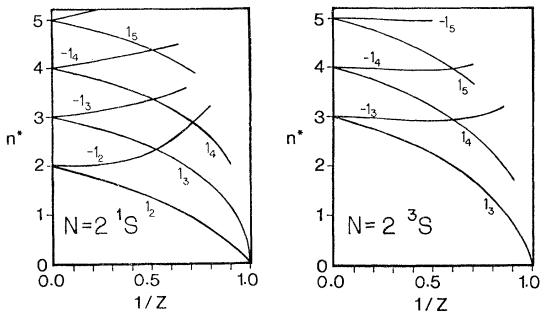


FIG. 1. $Z$ dependence of the DESB classification of hydrogenic CI $^{1,3}S$ states below the $N = 2$ threshold. $n^*$ is the effective quantum number in a Rydberg formula. Each curve is labeled with the DESB quantum numbers $K$ and $n$, as $K_n$.

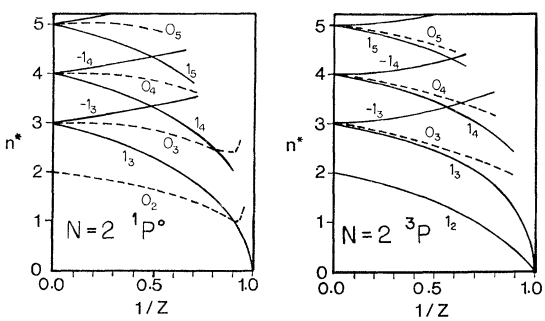


FIG. 2. $Z$ dependence of the DESB classification of the hydrogenic CI $^{1,3}P^\circ$ states below the $N = 2$ threshold. See Fig. 1 for notation.

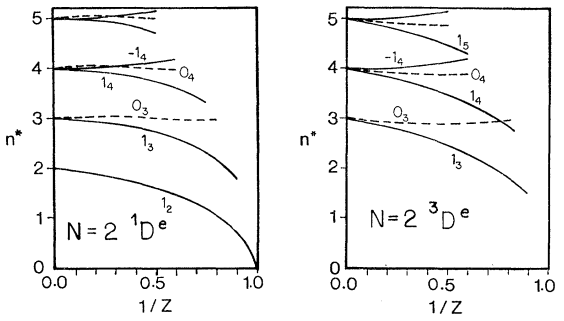


FIG. 3. $Z$ dependence of the DESB classification of the hydrogenic CI $^{1,3}D^e$ states below the $N=2$ threshold. See Fig. 1 for notation.

DESB components shows a stronger mixing, and suggests that the actual position of the crossing may lie at $Z<2$. The two states have not been resolved experimentally,[5] appearing at 64.14 eV above the ground state of He. In any case it is clear that regions of avoided crossings must be examined with care since they affect calculated properties of the physical states (integer $Z$). A significant number of crossings have been found near $Z=2$.

In Tables III and IV appear the energies, DESB classifications, and AI widths of helium $^1P^\circ$ states below the $N=3$, 4, and 5 thresholds. For $N=3$ there are five Rydberg series projected out in the DESB. Our CI energies are quite close to those of Oberoi.[21] The $K=+1_n$ states correspond to the experimental uv absorption results, as predicted by our $K=N-2$ "selection rule." Avoided crossings with the $K=-1_{n-1}$ states (see Fig. 4) show that the experimental spectrum probably results from an overlapping of the +1 and −1 series. Our calculated AI widths support this interpretation. The analysis for the $N=4$ $^1P^\circ$ state is similar, except that a "crossing" of the $1_5$ and $2_5$ curves just below $Z=2$ causes a slight mixing of the states. Since the $1_5$ and $2_5$ states are degenerate at infinite $Z$, "near

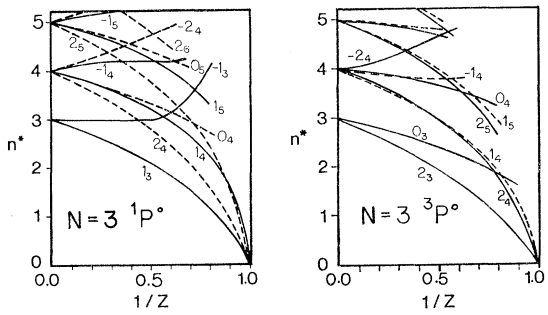


FIG. 4. $Z$ dependence of the DESB classification of the hydrogenic CI $^{1,3}P^\circ$ states below the $N=3$ threshold. See Fig. 1 for notation.

TABLE II. Comparison of the group theoretical DESB classification of two $N=2$ $^1P^\circ$ helium states at 64.1 eV in our hydrogenic CI basis vs the more extensive hydrogenic CI basis of Lipsky and Russek, to illustrate the dependence of the "avoided crossing" of the states (see Fig. 1) upon the method of calculation.

| | $K_n$ | $E$[a] | Fraction of normalization $K=+1$ | $K=0$ | $K=-1$ |
|---|---|---|---|---|---|
| This paper | $1_4$ | 64.14 | 0.9191 | 0.0235 | 0.0574 |
| | $-1_3$ | 64.17 | 0.0642 | 0.0094 | 0.9263 |
| Lipsky and Russek[b] | $-1_3$ | 64.11 | 0.2940 | 0.0311 | 0.6718 |
| | $1_4$ | 64.12 | 0.6862 | 0.0038 | 0.3077 |

[a] Energy above the ground state of helium in eV.
[b] Reference 20.

degeneracy" is a more suitable description of this type of interaction. The $K=+2$ Rydberg series is identified with the experimental results, as predicted by the $K=N-2$ rule for dipole excitation.

No experimental results are currently available for the $^1P^\circ$ states with $N=5$. A possible explanation for this is found in the observation that our calculated energy for the lowest state is $n^*=3.272$, which lies *below* the $N=4$ threshold of helium at $N^*=3.333$. Autoionization to the $N=4$ continuum channels $\overline{4LkL'}$ $^1P^\circ$ is thus forbidden, resulting in our comparatively narrow calculated width of 0.006 eV. Extrapolation of the experimental effective quantum numbers for the lower threshold $^1P^\circ$ states gives $n^*\cong 3.30$ at $N=5$, although the possibility that the state lies above threshold cannot be ruled out at present. If indeed experiment eventually does show that it lies above threshold, then the Feshbach $Q$-space as it is usually defined will have to be modified so as to allow the calculation of partial decay widths to the $N=4$ continuum. This phenomenon of Rydberg envelopes overlapping with each other is very common for the high-energy doubly-excited states, and has gone unrecognized until now. In fact at infinite $Z$ it is easily seen that the $N$th nonrelativistic Rydberg envelope overlaps with the $(N-1)$th envelope for all $N>3$. For lower $Z$, the overlappings occur at higher values of $N$.

For comparison with the $^1P^\circ$ results, the $^3P^\circ$ helium states for $N=3$ are presented in Table III. As in the previous examples, each state is seen to be characterized very well by $K$ and $T$. The $K_n=2_4$ and $1_4$ states are nearly degenerate at $Z=2$ in the hydrogenic DESB (see Fig. 4), causing a heavy mixing between them. This mixing accounts for the broadness of the calculated autoionization width for the $1_4$ state. The variational calculation of Chung[22] indicates that the actual ordering of the two states may be reversed from that shown in

Table III, but unfortunately no autoionization widths were reported. The widths of higher states of the $K=2$, 1 series suggest that the $2_4$ width is probably closer to 0.05 eV, but the near degeneracy of the states would make any future observation of their relative energies unlikely. The occurrence of this near degeneracy at $Z \cong 2$ is similar to the crossing of the $^1P^\circ$ $K=1_5$ and $2_5$ states below the $N=4$ threshold. This type of "inversion" near $Z=2$ of states degenerate at infinite $Z$ has been found in other Rydberg series of different $L$ and $\pi$ symmetries. It is apparently due to a difference in the $Z$ dependence of correlation effects associated with the inner and outer regions of the wave function. For the positive ions ($Z>2$) the wave functions are compact, while for the negative ions ($Z<2$) they are more diffuse. It is not fully understood at present why near degeneracies in the neutral atom occur only for certain pairs of DESB states, and not for others.

## V. DESB CLASSIFICATION OF $H^-$ ENERGIES

The $H^-$ ion must be analyzed separately from isoelectronic species with $Z>1$ since the weakness of the long range attractive forces does not ensure the existence of an infinite number of states in each "series." For instance, the singly-excited Rydberg series $1snL$ ($n \geq 2$) collapse into degeneracy at the $N=1$ threshold when $Z=1$.

The DESB classification of doubly-excited $H^-$ is dependent upon a large number of avoided crossings in the $n^*$ vs $Z^{-1}$ curves as $Z \to 1$. We find in all cases that only doubly-excited CI states with $K>0$ remain "bound" relative to the $N=2$, 3, and 4 thresholds, reflecting the favorable angular correlation in DESB states with $K>0$.

The most interesting example of this effect is seen in the $^1P^\circ$ curves in Fig. 2. The $K=0_2$ curve corresponds at large $Z$ to the configuration $2s2p$ $^1P^\circ$. Due to an avoided crossing at $Z^{-1} \cong 0.9$, however, it is the $K=+1_3$ state which lies below threshold in $H^-$. The crossing of the $0_2$ and $1_3$ states is not widely recognized. It explains for instance why Drake and Dalgarno[23] did not calculate a $^1P^\circ$ state below threshold at $Z=1$ in their $1/Z$ perturbation energy expansion for the $2s2p$ $^1P^\circ$ configuration. Our calculations are the first to show the explicit $Z$ dependence of this crossing, although evidence

TABLE III. Comparison of group theoretical DESB classification of the $N=3$, $^{1,3}P^\circ$ hydrogenic CI states with calculated and experimental results for helium. See also Fig. 4 at $Z=2$.

| | This work | | $n^*$ | | | | AI width (eV) | |
|---|---|---|---|---|---|---|---|---|
| | $K_n$ | DESB fraction | This work | Oberoi[a] | Chung[b] | Expt.[c] | This[d] work | Expt.[e] |
| $^1P^\circ$ | $1_3$ | 0.9951 | 2.109 | 2.100 | 2.098 | 2.125 | 0.151 | 0.132±0.014 |
| | $2_4$ | 0.9980 | 2.806 | 2.800 | 2.800 | | 0.560(−3) | |
| | $-1_3$ | 0.9273 | 3.011 | 2.879 | 2.872 | | 0.677(−1) | |
| | $1_4$ | 0.9686 | 3.245 | 3.198 | 3.198 | 3.240 | 0.476(−1) | |
| | $0_4$ | 0.9857 | 3.347 | 3.316 | 3.323 | | 0.927(−3) | |
| | $2_5$ | 0.9942 | 3.779 | 3.768 | 3.768 | | 0.342(−3) | |
| | $-1_4$ | 0.8266 | 4.190 | 4.137 | 4.153 | | 0.246(−1) | |
| | $1_5$ | 0.8390 | 4.260 | 4.199 | 4.206 | 4.25 | 0.171(−1) | |
| | $0_5$ | 0.9666 | 4.411 | 4.387 | 4.404 | | 0.412(−3) | |
| | $-2_4$ | 0.9740 | 4.741 | 4.641 | 4.694 | | 0.111(−3) | |
| | $2_6$ | 0.9892 | 4.765 | ••• | 4.751 | | 0.211(−3) | |
| | $1_6$ | 0.8840 | 5.430 | 5.224 | 5.231 | 5.26 | ••• | |
| | $-1_5$ | 0.8659 | 5.285 | | 5.272 | | 0.015 | |
| $^3P^\circ$ | $2_3$ | 0.9987 | 1.970 | 1.965 | 1.964 | | 0.976(−1) | |
| | $0_3$ | 0.9935 | 2.419 | 2.379 | 2.374 | | 0.490(−1) | |
| | $1_4$ | 0.5353 | 2.980 | 2.941 | 2.939 | | 0.232(−1) | |
| | $2_4$ | 0.5350 | 2.984 | 2.971 | 2.972 | | 0.278(−1) | |
| | $0_4$ | 0.9791 | 3.666 | 3.625 | 3.622 | | 0.130(−1) | |
| | $-1_4$ | 0.9743 | 3.774 | 3.711 | 3.737 | | 0.117(−3) | |
| | $2_5$ | 0.9824 | 3.939 | 3.883 | 3.881 | | 0.248(−1) | |
| | $1_5$ | 0.9765 | 4.008 | 3.994 | 3.998 | | 0.402(−3) | |
| | $-2_4$ | 0.8730 | 4.684 | 4.591 | 4.654 | | 0.389(−3) | |
| | $0_5$ | 0.9381 | 4.711 | 4.663 | 4.692 | | 0.641(−2) | |
| | $-1_5$ | 0.8755 | 4.848 | | 4.820 | | 0.698(−4) | |
| | $2_6$ | 0.9749 | 4.938 | | 4.871 | | 0.160(−1) | |

[a] Reference 21.
[b] Reference 22.
[c] Madden and Codling, Ref. 5.
[d] $(-M)$ indicates $(0.1)^M$
[e] Reference 6.

TABLE IV. Comparison of group theoretical DESB classification of the $N=4, 5$, $^1P^o$ hydrogenic CI states with calculated and experimental results for helium. Note the avoided crossing interaction at $N=4$, $n^*=3.76$. $N=5$ states with $K<-1$ lie at higher energies and could not be included.

| | $K_n$[a] | DESB fraction[a] | $n^*$[a] | Width(eV)[a] | Other $n^*$[c] |
|---|---|---|---|---|---|
| $N=4$ | $2_4$ | 0.9970 | 2.680 | 0.046 | 2.675, 2.717 |
| | $0_4$ | 0.9842 | 3.131 | 0.124 | 3.128 |
| | $3_5$ | 0.9991 | 3.380 | 0.226(−3)[b] | 3.377 |
| | $1_5$ | 0.7495 | 3.756 | 0.64(−2)[b] | 3.745 |
| | $2_5$ | 0.7493 | 3.761 | 0.023 | 3.756, 3.77[d] |
| | $3_6$ | 0.9973 | 4.325 | 0.16(−3)[b] | 4.320 |
| | $0_5$ | 0.9322 | 4.407 | 0.051 | 4.403 |
| | $-1_5$ | 0.9654 | 4.579 | 0.148(−2)[b] | 4.579 |
| | $2_6$ | 0.9600 | 4.738 | 0.020 | 4.717, 4.75[d] |
| | $-2_4$ | 0.8571 | 4.787 | | 4.783 |
| | $1_6$ | 0.9726 | 4.820 | | |
| $N=5$ | $3_5$ | 0.9977 | 3.272 | 0.56(−2) | |
| | $1_5$ | 0.9906 | 3.595 | 0.054 | |
| | $4_6$ | 0.9994 | 3.971 | | |
| | $2_6$ | 0.9971 | 4.273 | | |
| | $3_6$ | 0.9924 | 4.324 | | |
| | $-1_5$ | 0.9519 | 4.344 | | |
| | $0_6$ | 0.9834 | 4.820 | | |
| | $1_6$ | 0.9828 | 4.851 | | |
| | $4_7$ | 0.9927 | 5.228 | | |

[a] This work.
[b] $(-M)$ indicates $(0.1)^M$.
[c] Oberoi, Ref. 21.
[d] Madden and Codling, experiment, Ref. 5.

for the phenomenon was cited by Macek and Burke.[24] Comparison of our results with the analysis of $H^-$ by these authors shows that our $K=0_2$ $^1P^o$ state (at 10.222 eV) may actually correspond to a shape resonance which they identify at 10.222 eV. By extrapolating Drake and Dalgarno's $2s2p$ $^1P^o$ energies for $Z \geq 2$ down to $Z=1$, we estimate that their method should also predict a resonance above threshold at $10.3 \pm 0.1$ eV.

In the $^3P^o$ series the $2s2p$ configuration corresponds at large $Z$ to the $K=1_2$ DESB state, which remains below the $N=2$ threshold as $Z \to 1$. A summary of the $N=2$ DESB classification for $H^-$ appears in Table V for comparison with other variational[25-28] energies, close-coupling resonances,[29,30] and with experiment.[31-34] All states below threshold have $K=+1$. A similar presentation of calculated[21,22,35] and experimental[36] results in Table VI for $N=3$ shows two types of autoionizing states, with either $K=+2$ or $K=+1$, but widths for the states are now known.

In general the $H^-$ states (for each threshold) with $K>0$ exhibit the strongest binding tendencies, while those with $K<0$ lie well above threshold in our CI approximation and do not appear to represent physical states. The lowest energy states with $K=0$ do exhibit a weak tendency to bind, and as our identification of the $K=0_2$ $^1P^o$ state at 10.22 eV indicates, they may correspond to shape resonances. This interpretation of our results is supported by the fact that both the $1s^2\,^1S$ and $2p^2\,^3P^e$ states have DESB representations with $K=0$, and both are "bound" relative to their respective ionization thresholds. In addition both the $1sns$ $^1S$

TABLE V. Group-theoretical "doubly-excited symmetry basis" classification of $N=2$, $H^-$ hydrogenic CI states and comparison with other theoretical and experimental energies.

| | | This work | Energy (eV) Theory | | | | Experiment | |
|---|---|---|---|---|---|---|---|---|
| $^{2S+1}L^\pi$ | $K_n$ | DESB normalization fraction | This work[a] | O'Malley and Geltman[b] | Bhatia *et al.*[c] | Burke *et al.*[d] | McGowan *et al.*[e] | Sanche and Burrow[f] |
| $^1S$ | $1_2$ | 0.9955 | 9.592 | 9.559 | 9.556 | 9.560 | 9.56 ± 0.010 | 9.558 ± 0.010 |
| | $1_3$ | 0.9997 | 10.178 | 10.178 | 10.175 | 10.178 | | |
| $^3S$ | $1_3$ | 0.9996 | 10.150 | 10.149 | 10.145 | 10.150 | | |
| $^1P^o$ | $1_3$ | 0.9876 | 10.178 | 10.178 | | 10.177 | | |
| | $0_2$ | 0.9218 | 10.222[g] | | | 10.222 | 10.29 ± 0.02 | |
| $^3P^o$ | $1_3$ | 0.9978 | 9.763 | 9.727 | 9.724 | 9.740 | 9.71 ± 0.03 | 9.738 ± 0.010 |
| | $1_4$ | 0.9797 | 10.194 | 10.198 | | | | |
| $^1D^e$ | $1_2$ | 0.9970 | 10.158 | | 10.119 | 10.125 | 10.13 ± 0.015 | 10.128 ± 0.010 |

[a] Using 1 a.u. = 27.2070 eV, with respect to the ground state of hydrogen.
[b] Reference 25.
[c] References 26–28.
[d] Close-coupling plus correlation, Refs. 29 and 30.
[e] References 31–33.
[f] Reference 34.
[g] Possible shape resonance, see text and also Table VII.

and $2pnp\ ^3P^e$ Rydberg series (for $Z>1$) collapse to threshold as $Z \to 1$, indicating the weakness of the long-range binding forces in the $K=0$ states. A summary of our lowest energy $H^-$ CI states with $K=0$ for $N=2, 3, 4$ is given in Table VII for comparison with the experimental shape resonances of McGowan *et al.*[36] For $N=2, 3$ the agreement is good, although our energies tend to be lower than the experimental values. This is probably due to the fact that we do not include any interactions with the continuum. No experimental $N=4$ shape resonance energies were reported.

It is informative to consider the problem of identifying the shape resonances by assuming that the quasiseparability of the Hamiltonian noted by Macek[19] in hyperspherical coordinates for He is valid also for $H^-$. The problem then reduces to a description of the motion along the coordinate $R=(r_1^2+r_2^2)^{1/2}$ in an effective potential $U_R$ obtained by integrating the wave equations with respect to the five hyperspherical angles. As $R \to \infty$, $U_R$ approaches the threshold limit of the Rydberg series of interest. In accordance with our preceding remarks, we have illustrated qualitatively in Fig. 5 possible shapes of $U_R$ for describing the features of the DESB states with $K>0$, $K=0$, and $K<0$, respectively. The $K>0$ potential can support an infinite number of states, each of which can autoionize to continua of lower thresholds. The $K<0$ potential cannot support any doubly-excited states, and is probably purely repulsive. For $K=0$ we have illustrated a possible "shape" potential and have indicated two types of states within the well. In case (A), the state lies below threshold and undergoes autoionization to lower threshold channels. In case (B), however, the state may decay directly to a lower threshold channel as in (A), or it may penetrate the repulsive barrier and decay to a continuum channel which is only open above threshold. Although these effective potentials describe our results qualitatively, it remains to be seen whether or not the exact $U_R$ are capable of

TABLE VI. Group theoretical "doubly-excited symmetry basis" classification of $N=3$, $H^-$ hydrogenic CI states and comparison with other theoretical and experimental energies.

| | | This work | Energy (eV) Theory[a] | | | | Experiment |
|---|---|---|---|---|---|---|---|
| $^{2S+1}L^{\pi}$ | $K_n$ | DESB normalization fraction | This paper | Oberoi[b] | Burke *et al.*[c] | Chung[d] | McGowan *et al.*[e] |
| $^1S^e$ | $2_3$ | 0.9971 | 11.726 | 11.718 | 11.733 | | 11.65±0.03 |
| | $2_4$ | 0.9973 | 12.035 | 12.030 | 12.037 | | |
| $^3S^e$ | $2_4$ | 0.9990 | 12.002 | 11.998 | | | |
| | $2_5$ | 0.9992 | 12.079 | 12.074 | | | |
| $^1P^o$ | $1_3$ | 0.9915 | 11.923 | 11.905 | 11.915 | 11.904 | 11.89±0.02 |
| | $2_4$ | 0.9983 | 12.013 | 12.010 | | 12.010 | |
| | $2_5$ | 0.9534 | 12.084 | 12.077 | | 12.077 | |
| | $1_4$ | 0.9519 | 12.088 | 12.083 | | 12.085 | |
| $^3P^o$ | $2_3$ | 0.9974 | 11.755 | 11.746 | 11.764 | 11.746 | 11.77±0.02 |
| | $2_4$ | 0.9951 | 12.044 | 12.040 | 12.048 | 12.040 | |
| | $1_4$ | 0.9946 | 12.074 | 12.070 | | 12.071 | |
| $^1D^e$ | $2_3$ | 0.9977 | 11.820 | 11.809 | 11.819 | | {11.77±0.02, 11.89±0.02} |
| | $2_4$ | 0.9899 | 12.061 | 12.058 | | | |
| $^3D^e$ | $1_3$ | 0.9848 | 12.007 | 11.986 | | | |
| | $2_4$ | 0.9962 | 12.036 | 12.032 | | | |
| $^1P^e$ | $1_4$ | 0.9988 | 12.073 | | | | |
| $^3P^e$ | $1_3$ | 0.9946 | 11.917 | | | | |
| | $1_4$ | 0.9992 | 12.087 | | | | |
| $^1D^o$ | $1_3$ | 0.9967 | 11.998 | | | | |
| $^3D^o$ | $1_4$ | 0.9636 | 12.092 | | | | |
| $^1F^o$ | $2_4$ | 0.9930 | 12.069 | | | | |
| $^3F^o$ | $2_3$ | 0.9978 | 11.926 | | | | |
| | $2_4$ | 0.9805 | 12.083 | | | | |
| $^1G^e$ | $2_3$ | 0.9961 | 12.087 | | | | |

[a] Using 1 a.u. = 27.2070 eV, with respect to the ground state of hydrogen.
[b] Reference 21.
[c] Reference 35.
[d] Reference 22.
[e] Reference 36.

reproducing the observed shape resonances.

We note also that the exact relationship between our group theoretical classification of $H^-$ states and the familiar "dipole" classification[37,38] of angular mixings is not entirely clear at present, since the DESB accounts for some of the short-range Coulomb effects as well as the long-range effects. The advantage of using the DESB for the lower Rydberg series states is of course that the mixing coefficients are obtained *a priori* from Eq. (2).

## VI. COMPARISON OF PREDICTED AUTOIONIZATION "SELECTION RULES" WITH EXPERIMENT AND WITH CALCULATED WIDTHS FOR HELIUM

AI Rules I–III predict remarkably well the experimental and calculated AI properties of He. We discuss separately the important features of the classification for states below the $N=2$, 3, and 4 thresholds.

### A. $N=2$ states

We see immediately from Rule I that only $S^e$, $P^o$, and $D^e$ states are predicted to be AI-allowed, since $K$ is restricted to the values 0, ±1. The predicted AI properties are as follows:

(i) $S^e$. The configurations $2sns$, $2pnp$ give rise to the series $K=+1$, $-1$ and by Rule II only the $^1S$ series are AI-allowed. Rule III predicts that for both singlet and triplet series the $K=-1$ states will be the narrowest.

(ii) $P^o$. All three $K$ values are permitted for $L>0$, and the $P^o$ series result from mixing of the $2snp$, $2pns$, and $2pnd$ configurations. By Rules I and II only the $K=0$ $^1P^o$ and $K=1$ $^3P^o$ series are AI-allowed. Of the four AI-forbidden series the two $K=-1$ series will be the weakest by Rule III.

(iii) $D^e$. The six series in this case result from mixing of the $2snd$, $2pnp$, and $2pnf$ configurations. Rule II predicts that only the $K=1$ $^1D^e$ series (with lowest state $2p^2\,^1D^e$) is AI-allowed. Both $K=-1$ series are expected to be extremely weak since they are forbidden by Rule III and Rule I. In fact,

TABLE VII. Possible shape resonances for $N=2,3,4$ states of $H^-$ as determined from bound-state hydrogenic CI calculations and comparison with experiments. Only states with DESB quantum number $K=0$ are included, as discussed in Sec. V. All results are from this work unless otherwise indicated.

| | | | | Energy (eV) | |
|---|---|---|---|---|---|
| | $^{2S+1}L^{\pi}$ | $(K,T)_n$ | DESB Fraction of normalization | This paper[a] | Experiment[b] |
| $N=2$ | $^1P^o$ | $(0,1)_2$ | 0.9218 | 10.222 | 10.29± 0.02 |
| | $^3P^o$ | $(0,1)_3$ | 0.9658 | 10.223 | |
| | $^1D^e$ | $(0,1)_3$ | 0.9059 | 10.239 | |
| $N=3$ | $^1S^e$ | $(0,0)_3$ | 0.9818 | 12.107 | Broad resonance |
| | $^3S^e$ | $(0,0)_4$ | 0.9987 | 12.117 | at 12.06± 0.04, |
| | $^1P^o$ | $(0,0)_4$ | 0.9826 | 12.124 | and structure at |
| | $^3P^o$ | $(0,0)_3$ | 0.8421 | 12.122 | 12.16± 0.05, |
| | $^1D^e$ | $(0,2)_3$ | 0.9502 | 12.113 | 12.23± 0.05, and |
| | $^3D^e$ | $(0,2)_4$ | 0.9610 | 12.118 | 12.35± 0.05. |
| | | $(0,0)_4$ | 0.9561 | 12.137 | |
| | $^1F^o$ | $(0,2)_4$ | 0.9476 | 12.144 | |
| | | $(0,0)_4$ | 0.8400 | 12.160 | |
| | $^3F^o$ | $(0.,2)_4$ | 0.9407 | 12.144 | |
| | | $(0,0)_4$ | 0.9339 | 12.159 | |
| | $^1D^o$ | $(0,2)_4$ | 0.9633 | 12.118 | |
| | $^3D^o$ | $(0,2)_3$ | 0.9560 | 12.112 | |
| $N=4$ | $^1P^o$ | $(0,1)_4$ | 0.9776 | 12.773 | |
| | $^3P^o$ | $(0,1)_5$ | 0.7111 | 12.787 | |
| | $^1D^e$ | $(0,1)_5$ | 0.9428 | 12.801 | |
| | $^3D^e$ | $(0,1)_4$ | 0.9666 | 12.795 | |
| | $^1P^e$ | $(0,1)_5$ | 0.9789 | 12.787 | |
| | $^3P^e$ | $(0,1)_4$ | 0.9816 | 12.771 | |
| | $^1D^o$ | $(0,1)_4$ | 0.9772 | 12.793 | |
| | $^3D^o$ | $(0,1)_5$ | 0.9675 | 12.800 | |

[a] Using 1 a.u. = 27.2070 eV, with respect to the ground state of hydrogen.
[b] McGowan *et al.*, Ref. 36.

the lowest $K=-1$ series member is the $n=4$ state. The remaining $^3D^e$ series are also AI-forbidden, but Rule III is not sensitive enough to the structure of the DESB wave functions to predict an ordering of their widths. The lowest energy DESB wave functions for the $K=1$ and $K=0$ series are respectively $\sqrt{\frac{1}{3}}(2s3d)-\sqrt{\frac{2}{3}}(2p3p)$ and $\sqrt{\frac{2}{3}}(2s3d)+\sqrt{\frac{1}{3}}(2p3p)$ $^3D^e$. The Pauli exclusion effect prevents the $2p3p$ configuration from contributing significantly to the width, while in the $2s3d$ configuration it is the weakness of the $3d$ radial function in the nuclear region which inhibits autoionization. The penetration of the $2s$ orbital causes the $2s3d$ configuration to dominate slightly in the autoionization process, making the $K=0$ series broader than the $K=1$ series.

The energies and widths of the $N=2$ threshold $S^e$, $P^o$, and $D^e$ helium states are too familiar[18,26-28] to warrant appearance here, and the DESB energy classification was displayed in Figs. 1-3. In general the predicted AI trends are in excellent agreement with experiment and calculations. The lowest-energy states for each $L$ have widths >0.02 eV, while the narrowest AI-forbidden widths ($K=-1$ for all except $^1S^e$) are nearly $10^{-4}$ times smaller. Our calculated widths are surprisingly good considering the simplicity of our method, and are significantly better than those of Altick and Moore[15]

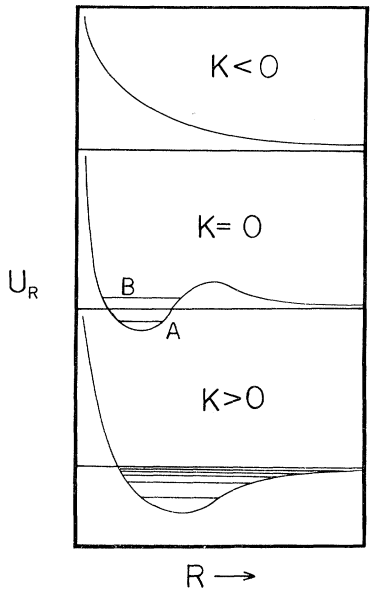


FIG. 5. Three possible effective potentials along the hyperspherical coordinate $R=(r_1^2+r_2^2)^{1/2}$ consistent with the group theoretical DESB classification of $H^-$ hydrogenic CI states, for the quantum number $K<0$, $=0$, and $>0$. *A* and *B* represent an autoionizing state and a shape resonance, respectively for $K=0$. No autoionizing states occur for $K<0$, while for $K>0$ the attractive well can support an infinite number of states.

for the $^{1,3}D^e$ states due to our larger CI basis. Our $K=0_2$ $^1P^o$ width ($=2s2p$ $^1P^o$ in the older notation) is $\Gamma=0.036$ eV, which is comparable to the value 0.037 eV calculated by Bhatia and Temkin,[27] and to the experimental width[5] 0.038 eV. A detailed compilation of results is contained in Ref. 17.

To test the prediction that states with $L>2$ are AI-forbidden, an additional CI calculation of the $^1F^o$ states was made. The lowest-energy states $K_n=+1_3, 0_4, -1_5$ of each DESB symmetry are respectively: 63.84 (width $=0.44\times10^{-3}$), 64.55 (width $=0.29\times10^{-6}$) and 64.87 (width $=0.19\times10^{-7}$) in eV. Each is narrow as expected.

### B. $N=3$ states

Because of the increased complexity of the DESB classification for $N>2$ we analyze in detail the $^{1,3}P^o$ AI widths presented in Table III. There are a total of ten singlet and triplet $P^o$ series corresponding to configurational mixing of the $3snp$, $3pns$, $3pnd$, $3dnp$, and $3dnf$ series. The $(K,T)$ values labeling the DESB series are (2,0), (1,1), (0,0), (-1,1), and (-2,0). By setting $n=3$, we see from Rule I that only values of $K\geq-1$ are predicted to be AI-allowed. The exchange restrictions imposed by Rule II further determine that for $^1P^o$ only the (1,1) and (-1,1) series can be AI-allowed, and the (2,0), (0,0) series are AI-allowed for $^3P^o$. Rule III predicts that the (1,1) $^1P^o$ series will be broader than the (-1,1) series. These predictions describe the calculated widths extremely well. In addition, our value of 0.151 eV for the width of the lowest $K=1$ $^1P^o$ state is in excellent agreement with the experimental value of $0.132\pm0.014$ determined recently by Dhez and Ederer.[6]

The $^1S$ states appear in Table VIII. All the singlet states are predicted to be AI-allowed by Rules I and II. Agreement with these predicted widths is seen. The $K=-2$ series is sufficiently narrow so as to be classified as AI-forbidden, and in fact was not found in the close-coupling calculations. The narrowness of this series supports Rule III.

The $^{1,3}P^e$ states are displayed in Table IX. The triplet states are predicted to be broad while the singlet states should be narrow, but the $K=-1$ series are expected to be weak from Rule III. The widths confirm this prediction, and in fact the $K=-1$ states are the narrowest of the $N=3$ states we calculated. This narrowness does not exclude the possibility that they may appear in beam-foil spectra, but no such observation has yet been made. Comparison with the variational energies of Holøien and Midtdal[39] is favorable, with our hydro-

TABLE VIII. Energies, autoionization widths, and DESB classification of the $N=3$, $^1S^e$ helium states. Rules I–III predict the $K=2$ and $K=0$ states to be broadest.

| This work | | Effective quantum number, $n^*$ | | | | | Width (eV) | |
|---|---|---|---|---|---|---|---|---|
| $K_n$ | DESB Fraction | This work | Oberoi[a] | CC[b] | TDM[c] | Holøien[d] | This work | CC[b] |
| $2_3$ | 0.9982 | 1.950 | 1.944 | 1.952 | 1.949 | 1.968 | 0.083 | 0.086 |
| $0_3$ | 0.9887 | 2.338 | 2.307 | 2.301 | 2.316 | 2.370 | 0.146 | 0.225 |
| $2_4$ | 0.9975 | 2.946 | 2.905 | 2.942 | 2.919 | 2.997 | 0.046 | 0.048 |
| $0_4$ | 0.9861 | 3.575 | 3.500 | 3.560 | 3.507 | 3.770 | 0.037 | 0.069 |
| $-2_3$ | 0.9792 | 4.304 | 3.767 | ••• | 3.786 | 4.825 | 0.000 32 | ••• |
| $2_5$ | 0.9966 | 3.898 | 3.805 | 3.882 | 3.859 | 3.884 | 0.023 | 0.025 |
| $0_5$ | 0.9629 | 4.618 | 4.549 | 4.558 | 4.555 | ••• | 0.018 | 0.030 |
| $-2_4$ | 0.9686 | 5.305 | 4.769 | ••• | 4.775 | ••• | ••• | ••• |
| $2_6$ | 0.9942 | 4.885 | 4.807 | 4.865 | 4.828 | ••• | 0.015 | ••• |

[a] Reference 21.

[b] Close coupling calculation, S. Ormonde and L. Lipsky, quoted in Ref. d below. See also Ref. c below.

[c] Truncated diagonalization method, S. Ormonde, W. Whitaker, and L. Lipsky, Phys. Rev. Lett. 19, 1161 (1967). Hydrogenic basis set, but with coupling to higher Rydberg envelopes included.

[d] E. Holøien and J. Midtdal, J. Phys. B 4, 32 (1971).

genic CI results giving slightly lower energies.

A summary of lowest energy AI-allowed $S$, $P$, $D$, $F$, $G$ states appears in Table X. While no general trend of the total widths of these states is readily discernible, a comparison of the partial decay widths for the $1skL$ continuum channel does show that states with the largest values of $K$ and $T$ autoionize most rapidly. This agrees with the prediction of Rule III. AI to the higher continuum channels depends upon more diffuse properties of the doubly-excited wave function not associated with electron penetrability arguments. Nevertheless, Rule III predicts quite well relative widths of series within a given $L$, $\pi$ symmetry.

### C. $N=4$ states

Rules I and II continue to describe the broad and narrow characteristics of the $N=4$ states quite well. Rule III, however, does not predict the total width properties as well as it did for the $N=2$ and 3 states. The reason for this is twofold. First, the wave functions of the $N=4$ doubly-excited states are diffuse, and AI goes preferentially to the $N=3$ continuum channels. The two-electron penetrability into the nuclear region can no longer be used exclusively to describe the relative autoionization rates. On the other hand, for decay to the $N=1$ and $N=2$ continuum channels we do expect Rule III to predict correctly the width properties of the DESB states.

Our calculated widths indicate that a second, more fundamental reason for the apparent breakdown of Rule III for $N=4$ states is that the autoionization rates have a strong energy (i.e., the energy of the ejected electron) dependence through Eq. (6) that we have not accounted for in the derivation of the rules. As we noted in Sec. IV, at high values of $N$ the lowest-energy doubly-excited states drop below the $(N-1)$ threshold thus closing off these continuum channels to autoionization in our width calculations. For $N=4$ the lowest-energy states ($K>0$) have an effective Rydberg quantum number $n^*\sim 2.6$, which is above the $N=3$ threshold of $He^+$ at $n^*=2.268$ but close enough so that the decay to the $N=3$ channels is weaker than that from the higher-energy states with $K<0$. Thus for $N\geq 4$, Rule III is of use mainly for describing the

TABLE IX. Energies, autoionization widths, and DESB classification of the $N=3$, $P^e$ helium states for comparison with DESB width selection rules. Predicted broadest states are indicated by an asterisk (*). All results are from this paper unless otherwise specified.

| | | | $n^*$ | | |
|---|---|---|---|---|---|
| | $K_n$ | DESB% | This paper | Holøien & Midtdal[a] | Width (eV) |
| $^1P^e$ | $1_4$ | 99.89 | 2.977 | 2.977 | 0.336(−3) |
| | $-1_4$ | 99.65 | 3.733 | 3.676 | 0.922(−5) |
| | $1_5$ | 99.67 | 4.001 | 4.027 | 0.212(−3) |
| | $-1_5$ | 99.65 | 4.787 | 4.964 | 0.658(−5) |
| $^3P^e$ | $1_3$ | 99.67 | 2.094 | 2.074 | 0.115* |
| | $-1_3$ | 99.39 | 2.860 | 2.696 | 0.428(−3) |
| | $1_4$ | 99.37 | 3.215 | 3.248 | 0.455(−1)* |
| | $-1_4$ | 98.67 | 4.091 | 4.088 | 0.233(−7) |
| | $1_5$ | 98.61 | 4.220 | 4.722 | 0.224(−1)* |
| | $-1_5$ | 99.09 | 5.159 | 9.404 | 0.689(−5) |

[a] Multiconfigurational energy bound method, Ref. 39.

relative autoionization rates to the inner continuum channels. Explicit inclusion of these energy effects into our selection rules has not been considered. Applicability of Rule III to the partial AI widths of the $N=1$ and 2 continua is demonstrated in Table XI for the $^3P^o$ and $^1D^e$ states. The $N=4$ states with $K<-1$ were found to lie very high in energy and could not be included. Additional widths for the $^{1,3}P^e$ states also appear in Table XI.

## VII. DISCUSSION

The DESB quantum numbers $K$ and $T$ are remarkably useful for classifying the energy spectrum and autoionization widths of the doubly-excited helium spectrum. The relative simplicity of our hydrogenic CI calculations in comparison with more sophisticated calculations has allowed us to extend the classification of energy levels to higher thresholds ($N>2$) and to the entire isoelectronic sequence with a minimum of effort. Several important results were noted and are summarized below.

(i) The isoelectronic spectrum contains a number of "avoided crossings" of two (or more) states as $Z$ is varied continuously, and many of the crossings occur near $Z=2$. The exact determination of the crossings should be of concern in future calculations since the excitation and autoionization properties of the separate states can change considerably in the crossing region. Further analysis may show why some pairs of $(K, T)$ combinations interact more strongly than others, especially near $Z=2$. The intriguing possibility also arises that in a more complete basis set some of the crossings may be *exact*. This situation is likened to the exact potential energy curve crossings in the hydrogen molecule ion as the internuclear separation is varied.

(ii) It would be desirable to repeat our calculations using only subspaces of the CI basis diagonal in $K$ and $T$. This procedure may give a more realistic description of the crossings and would allow autoionization widths to be assigned to states in the crossing regions.

(iii) For $H^-$ our CI states with $K=0$ appear to describe shape resonances, although no rigorous proof of this assertion was offered. Further investigation of these states (including lifetimes) is needed, as well as the possibility that some states with $K<0$ may also correspond to shape resonances.

(iv) The discovery of overlapping Rydberg "envelopes" is of interest because it implies that there exist isolated states from one envelope (e.g., $N=5$) imbedded in Rydberg series of another envelope (e.g., $N=4$). We have not considered the interaction of different Rydberg envelopes in our cal-

TABLE X. Summary of calculated autoionization widths and ($1skL$) partial widths of the $N=3$ helium states for comparison with the DESB width selection rules. Only states with both electrons in the $N=3$ shell are included.

| $^{2S+1}L\ (K,T)_n$ | $n^*$ This paper | $n^*$ CCC[a] | Width (eV) This paper | Width (eV) CCC[a] | Partial width $1skL$ |
|---|---|---|---|---|---|
| $^1S^e\ (2,0)_3$ | 1.950 | 1.954 | 0.828(−1) | 0.825(−1) | 0.632(−2) |
| $^3P^o\ (2,0)_3$ | 1.970 | 1.978 | 0.976(−1) | 0.116 | 0.101(−2) |
| $^1D^e\ (2,0)_3$ | 2.028 | 2.040 | 0.242 | 0.154 | 0.338(−2) |
| $^3P^e\ (1,1)_3$ | 2.094 | | 0.115 | | 0 |
| $^1P^o\ (1,1)_3$ | 2.109 | 2.115 | 0.151 | 0.204 | 0.899(−3) |
| $^3F^o\ (2,0)_3$ | 2.133 | | 0.275(−1) | | 0.237(−3) |
| $^1D^o\ (1,1)_3$ | 2.174 | | 0.330(−1) | | 0 |
| $^3D^e\ (1,1)_3$ | 2.200 | | 0.542(−1) | | 0.112(−3) |
| $^1S^e\ (0,0)_3$ | 2.338 | 2.309 | 0.146 | 0.203 | 0.292(−3) |
| $^3D^o\ (0,2)_3$ | 2.336 | | 0.580(−1) | | 0 |
| $^1D^e\ (0,2)_3$ | 2.346 | | 0.115 | | 0.678(−3) |
| $^3P^o\ (0,0)_3$ | 2.419 | | 0.490(−1) | | 0.245(−4) |
| $^1G^e\ (2,0)_3$ | 2.428 | | 0.206 | | 0.101(−3) |
| $^3F^e\ (1,1)_3$ | 2.401 | | 0.628(−1) | | 0 |
| $^1F^o\ (1,1)_3$ | 2.488 | | 0.926(−1) | | 0.785(−3) |
| $^1D^e\ (0,0)_3$ | 2.786 | | 0.327(−1) | | 0.439(−3) |
| $^3P^e\ (-1,1)_3$ | 2.860 | | 0.428(−3) | | 0 |
| $^1P^o\ (-1,1)_3$ | 3.011 | | 0.677(−1) | | 0.276(−3) |
| $^1S^e\ (-2,0)_3$ | 4.304 | 4.320 | 0.322(−3) | | 0.214(−5) |

[a] P. G. Burke and A. J. Taylor, J. Phys. B 2, 44 (1969). Close coupling plus correlation calculations

TABLE XI. Energies, autoionization widths, and DESB classification of the $N=4$, $^3P^o$, $^1D^e$, and $^{1,3}P^e$ helium states for comparison with DESB width selection rules. * denotes the predicted broadest states.

| | This work | | $n^*$ | | This work | |
|---|---|---|---|---|---|---|
| | $K_n, (K,T)_n$ | DESB% | This work | Oberoi[a] | Total width (eV) | Partial width (eV)[b] |
| $^3P^o$ | $3_4$ | 99.89 | 2.569 | 2.565 | 0.252(−1) | 0.687(−2)* |
| | $1_4$ | 99.42 | 2.866 | 2.863 | 0.724(−1) | 0.244(−2)* |
| | $2_5$ | 99.85 | 3.520 | 3.517 | 0.314(−3) | 0.392(−5) |
| | $3_5$ | 99.73 | 3.556 | 3.543 | 0.206(−1) | 0.608(−2)* |
| | $-1_4$ | 96.43 | 3.710 | 3.708 | 0.574(−1) | 0.243(−3) |
| | $0_5$ | 98.49 | 4.034 | 4.033 | 0.162(−2) | 0.468(−5) |
| | $1_5$ | 97.87 | 4.062 | 4.057 | 0.329(−1) | 0.142(−2)* |
| | $3_6$ | 98.29 | 4.478 | 4.472 | 0.126(−1) | 0.372(−2)* |
| | $2_6$ | 98.41 | 4.514 | 4.516 | 0.420(−3) | 0.317(−4) |
| | $-1_5$ | 93.17 | 4.999 | 4.995 | 0.137(−1) | 0.400(−4) |
| $^1D^e$ | $3_4$ | 99.91 | 2.601 | 2.596 | 0.724(−1) | 0.187(−1)* |
| | $(1,2)_4$ | 97.82 | 2.842 | 2.838 | 0.792(−1) | 0.942(−2)* |
| | $(1,0)_4$ | 97.78 | 2.954 | 2.950 | 0.130 | 0.190(−2) |
| | $(-1,2)_4$ | 93.73 | 3.574 | 3.570 | 0.976(−1) | 0.410(−3) |
| | $2_5$ | 98.57 | 3.578 | 3.575 | 0.392(−2) | 0.111(−3) |
| | $3_5$ | 99.78 | 3.613 | 3.599 | 0.559(−1) | 0.157(−1)* |
| | $(1,2)_5$ | 96.61 | 4.021 | 4.014 | 0.368(−1) | 0.548(−2)* |
| | $(1,0)_5$ | 63.85 | 4.153 | 4.149 | 0.348(−1) | 0.381(−3) |
| | $0_5$ | 71.65 | 4.204 | 4.203 | 0.129(−1) | 0.275(−3) |
| | $(-1,0)_4$ | 72.65 | 4.290 | 4.288 | 0.242(−1) | 0.108(−2) |
| $^1P^e$ | $2_5$ | 99.90 | 3.518 | | 0.371(−4) | |
| | $0_5$ | 99.50 | 4.021 | | 0.118(−3) | |
| | $2_6$ | 99.90 | 4.511 | | 0.206(−4) | |
| $^3P^e$ | $2_4$ | 99.76 | 2.674 | | 0.359(−1)* | |
| | $0_4$ | 98.90 | 3.095 | | 0.886(−1)* | |
| | $2_5$ | 99.73 | 3.746 | | 0.226(−1)* | |
| | $0_5$ | 92.60 | 4.361 | | 0.225(−1)* | |
| | $-2_4$ | 90.80 | 4.653 | | 0.121(−1)[c] | |
| | $2_6$ | 98.79 | 4.722 | | 0.147(−1)* | |

[a] Reference 21.
[b] Partial AI decay width to the $1skL$ and $2lkl'$ continuum channels.
[c] Broad due to interaction with the $0_5$ state.

culations, but it is clear that they must be included for an accurate description of the energies and widths of the states involved.

While we have used the more transparent properties of the DESB coupling coefficients [Eq. (3)], a more systematic investigation of their properties may lead to the discovery of additional systematics in the spectra of heliumlike ions. For instance, a careful perusal of the DESB coefficients shows that there exists a one-to-one mapping of all states within a given Rydberg envelope of threshold $N$ and $\pi=(-)^L$ onto the Rydberg envelope of threshold $N-1$ and $\pi=(-)^{L+1}$. The spectra of these two types of states are found to be quite similar, but the group-theoretical implications of such congruences remain a mystery. Note for example, the similarity between the $1sns$ $^1S^e$ and the $2pnp$ $^3P^e$ Rydberg series. Also the $(3pnp)$:$(3dnd)$ $^{3,1}P^e$ DESB mixing coefficients are similar to those of the $(2sns)$:$(2pnp)$ $^{1,3}S^e$ DESB states [Eqs. (4) and (5)], and the $n^*$ vs $Z^{-1}$ curves of the states are qualitatively alike. Explanation of such similarities will increase our understanding of the DESB classification, and possibly lead to a more comprehensive description of the helium spectrum.

*Work supported by a grant from the U. S. NSF.

†NASA Predoctoral Trainee. Present address: Bell Telephone Laboratories, Murray Hill, N. J.

‡Alexander von Humboldt Senior Scientist Awardee, 1973–1974, West Germany.

[1]O. Sinanoğlu and D. R. Herrick, J. Chem. Phys. (to be published).

[2]W. Pauli, Z. Phys. 33, 879 (1925).

[3]J. W. Cooper, U. Fano, and F. Prats, Phys. Rev. Lett. 10, 518 (1963).

[4]U. Fano, in *Atomic Physics*, edited by V. W. Hughes, B. Bederson, V. W. Cohen, and F. M. J. Pichanick (Plenum, New York, 1969).

[5]R. P. Madden and K. Codling, Astrophys. J. 141, 364 (1965).

[6]P. Dhez and D. L. Ederer, J. Phys. B 6, L59 (1973).

[7]J. Simpson, S. Mielczarek, and J. Cooper, J. Opt. Soc. Am. 54, 269 (1964).

[8]S. M. Silverman and E. N. Lassettre, J. Chem. Phys. 40, 1265 (1964).

[9]M. E. Rudd, Phys. Rev. Lett. 13, 503 (1964); 15, 580 (1965).

[10]N. Oda, F. Nishimura, and S. Tahira, Phys. Rev. Lett. 24, 42 (1970).

[11]P. D. Burrow, Phys. Rev. A 2, 1774 (1970).

[12]H. G. Berry, J. Desesquelles, and M. Dufay, Phys. Lett. A 36, 237 (1971); and Phys. Rev. A 6, 600 (1972).

[13]H. G. Berry, I. Martinson, L. J. Curtis, and L. Lundin, Phys. Rev. A 3, 1934 (1971).

[14]J. P. Buchet, M. C. Buchet-Poulizac, H. G. Berry, and G. W. F. Drake, Phys. Rev. A 7, 922 (1973).

[15]P. L. Altick and E. N. Moore, Phys. Rev. Lett. 15, 100 (1965); P. L. Altick and E. N. Moore, Phys. Rev. 147, 59 (1966); P. L. Altick and E. N. Moore, Proc. Phys. Soc. (Lond.) 92, 853 (1967).

[16]H. Feshbach, Ann. Phys. (N.Y.) 19, 287 (1962); 5, 537 (1958).

[17]D. R. Herrick, Ph.D. thesis (Yale University, 1973).

[18]P. G. Burke and D. D. McVicar, Proc. Phys. Soc. 86, 989 (1965).

[19]J. Macek, J. Phys. B 1, 831 (1968).

[20]L. Lipsky and A. Russek, Phys. Rev. 142, 59 (1966).

[21]R. S. Oberoi, J. Phys. B 5, 1120 (1972).

[22]K. T. Chung, Phys. Rev. A 6, 1809 (1972).

[23]G. W. F. Drake and A. Dalgarno, Proc. Roy. Soc. (Lond.) A 320, 549 (1971).

[24]J. Macek and P. G. Burke, Proc. Phys. Soc. 92, 351 (1967).

[25]T. F. O'Malley and S. Geltman, Phys. Rev. A 137, 1344 (1965).

[26]A. K. Bhatia, A. Temkin, and J. F. Perkins, Phys. Rev. 153, 177 (1967).

[27]A. K. Bhatia and A. Temkin, Phys. Rev. 182, 15 (1969).

[28]A. K. Bhatia, Phys. Rev. A 6, 120 (1972).

[29]P. G. Burke, in *Advances in Atomic and Molecular Physics*, edited by D. R. Bates and I. Estermann (Academic, New York, 1968), Vol. 4, p. 173.

[30]A. J. Taylor and P. G. Burke, Proc. Phys. Soc. (Lond.) 92, 536 (1967).

[31]J. W. McGowan, E. M. Clarke, and E. K. Curley, Phys. Rev. Lett. 15, 917 (1965); 17, 66(E) (1966).

[32]J. W. McGowan, Phys. Rev. 156, 165 (1967).

[33]S. Ormonde, J. McEwen, and J. W. McGowan, Phys. Rev. Lett. 22, 1165 (1969).

[34]L. Sanche and P. D. Burrow, Phys. Rev. Lett. 29, 1639 (1972).

[35]P. G. Burke, S. Ormonde, and W. Whitaker, Proc. Phys. Soc. 92, 319 (1967).

[36]J. W. McGowan, J. F. Williams, and E. K. Curley, Phys. Rev. 180, 132 (1969).

[37]M. J. Seaton, Proc. Phys. Soc. 77, 174 (1961).

[38]M. Gailitis and R. Damburg, Proc. Phys. Soc. 82, 192 (1963).

[39]E. Holøien and J. Midtdal, J. Phys. B 5, 1111 (1972).